Macromolecules

pubs.acs.org/Macromolecules Article

Impact of Photoactive Monomer Location in Photoresponsive Block Copolymer/Ionic Liquid Solutions

Claire L. Seitzinger and Timothy P. Lodge*

Cite This: https://doi.org/10.1021/acs.macromol.2c02113 Read Online

ACCESS | Metrics & More | Article Recommendations | Supporting Information

ABSTRACT: By incorporating a photoactive moiety into a block polymer, the phase behavior can be controlled with light. Previous studies have looked at situating azobenzene, a common photoresponsive molecule, along the backbone of the polymer as a pendant group, and even as part of the solvent rather than along a comonomer. Here, we study the effect of the positioning of pendant azobenzene groups along the polymer backbone on the lower critical disorder−order transition of poly(methyl methacrylate)-*block*-poly(benzyl methacrylate) (PMMA-*b*-PBnMA, or MB) in the ionic liquid 1,3-dimethyl imidazolium bis(trifluoromethylsulfonyl)-imide. Using small-angle X-ray scattering and ultraviolet (UV)-irradiated small-amplitude oscillatory shear rheology, the placement of azobenzene statistically along the benzyl methacrylate backbone (MBsA) is compared to locating it as a midblock between the PMMA and the PBnMA (MAB) or as an end block after the PBnMA (MBA). Two concentrations of polymer in the ionic solvent were studied, 35 and 50 wt %. At 35 wt %, MBsA microphase-separated at 60 °C, MBA at 100 °C, and followed by MAB at 120 °C, a trend that was repeated at 50 wt %. MBsA was the only polymer to order onto a lattice at 35 wt %, forming hexagonally close-packed spheres. Both MBsA and MBA formed hexagonally packed cylinders at 50 wt %. MBsA consistently ordered onto a lattice over the temperature range of interest, while MBA only did so at 50 wt %, and MAB remained disordered at both concentrations. MBsA was also the only sample of the three to successfully transition reversibly between order and disorder with light. Therefore, adjusting the location of the azobenzene units within the thermo- and photoresponsive polymer solution significantly changes the overall behavior of the solutions and the ability to control that behavior with light and temperature.

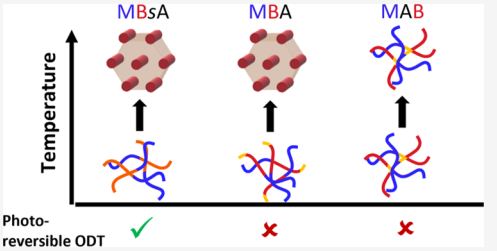

INTRODUCTION

Photoresponsive polymers have been studied for some time.[1−5] Light offers the possibility for both spatial and temporal control of the associated stimulus response. A common photoactive moiety to incorporate into a polymeric system is azobenzene.[6−12] It is popular due to its facile *trans*-to-*cis* isomerization under ultraviolet (UV) irradiation, which is readily reversible under visible light (Supporting Information, Scheme S1).[13] Additionally, the wavelength and lifetime of excitation/relaxation can be tuned by modifying the phenyl rings with a variety of substituents.[14] Azobenzene has been incorporated into polymer solutions as part of the backbone, as pendant groups, and even as part of the solvent.[15] Polymers with azobenzene in the backbone have been used to study azo bond behavior using infrared (IR) and UV/visible (UV/vis) absorption,[16−18] and have been used to induce shape changes in supramolecular nanofibers.[19] Azobenzene has also been attached to polymers as a pendant group, often via a methacrylate monomer that is then copolymerized and used to induce phase changes in solution.[11,20−22] Recently, Wang and co-workers have explored moving the photoactive moiety to the solvent rather than the polymer. They created an ionic liquid with an azobenzene-containing cation, 1-butyl-3-(4-phenylazobenzyl)imidazolium bis(trifluoromethylsulfonyl)-imide, and used it to control the phase separation of homopolymers in solution.[23−25] They have used this technique on both poly(2-phenylethyl methacrylate) and poly(benzyl methacrylate) (PBnMA).[10] They were also able to induce microphase separation with light in triblock copolymers of poly(2-phenylethyl methacrylate)-*b*-poly(methyl methacrylate)-*b*-poly(2-phenylethyl methacrylate).[26] Most of the changes investigated with the above materials involved micellization or order−disorder transitions controlled by light, without a particular focus on the ordered states formed. This leaves open the question of how the positioning of the photoactive monomer within the polymer influences the order−disorder transition temperature (T_{ODT}) and the ordered states formed.

Previous work from our group used the pendant group method of azobenzene incorporation, where a statistical copolymer of benzyl methacrylate (BnMA) and 4-phenylazophenyl methacrylate (AzoMA) was used as a photo- and

Received: October 14, 2022
Revised: December 10, 2022

https://doi.org/10.1021/acs.macromol.2c02113
Macromolecules XXXX, XXX, XXX−XXX

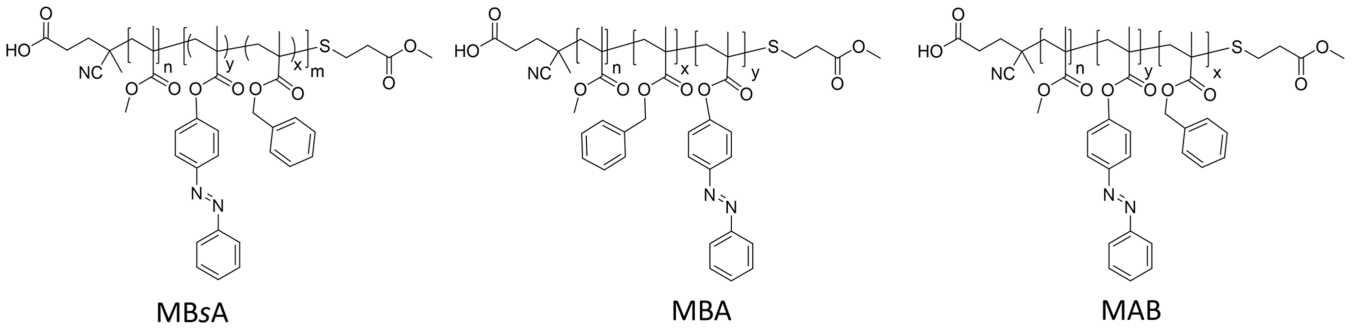

Figure 1. Structures of all three polymers investigated. MBsA has AzoMA statistically polymerized through the PBnMA block; MBA has a short AzoMA block at the end of the polymer; MAB has the AzoMA block in the middle of the polymer.

thermoresponsive block coupled with a poly(methyl methacrylate) (PMMA) block in a variety of ionic liquids.[20−22] A recent publication examined the effect of changing the block ratios between the PMMA and the responsive block, changing the AzoMA concentration, and changing the solvent selectivity by increasing the alkyl chain length in 1-alkyl-3-methyl imidazolium bis(trifluoromethylsulfonyl)imide.[20] The result of the block ratio modulation, between a symmetric polymer and a majority responsive block polymer, was a change in ordered state formed. The results of increasing AzoMA concentration from 5 to 12 mol % were to decrease the solubility of the polymer in the dark and to widen the temperature window over which photoresponse was possible. The solvent selectivity was found to be the best way to tune T_{ODT} across all of the samples.

To further explore the influence of azobenzene on the solution self-assembly, in this work, the effect of the location of the azobenzene along the polymer backbone on the lower critical ordering transition behavior in 1,3-dimethyl imidazolium bis(trifluoromethylsulfonyl) imide ([C_1mim][TFSI]) was investigated. Three options for AzoMA placement were explored: statistical (PMMA-*b*-P(BnMA-*stat*-AzoMA), MBsA), as an end-block (PMMA-*b*-PBnMA-*b*-PAzoMA, MBA), and as a midblock (PMMA-*b*-PAzoMA-*b*-PBnMA, MAB), as illustrated in Figure 1. Locating the azobenzene at the end of the backbone in MBA is expected to drive ordering from the end group. The *trans*-to-*cis* isomerization would result in a more drastic solubility change in the micelle core, impacting the photoactive behavior. PMMA-*b*-PAzoMA-*b*-PBnMA (MAB) would have an insoluble midblock, which could either draw chains together causing significant chain rearrangement upon the microphase separation of PBnMA, or could remain relatively soluble and shielded by the PMMA and PBnMA blocks in solution. In this study, all samples contain 5 mol % AzoMA and have an overall molar mass of ca. 20 kg/mol.

EXPERIMENTAL SECTION

Materials. 4-Cyano-4-[(dodecylsulfanylthiocarbonyl)sulfanyl]-pentanoic acid, 4,4′-azobis(4-cyanovaleric acid), tris(2-carboxyethyl) phosphate hydrochloride, *n*-propylamine, and methyl acrylate were used as purchased from Sigma-Aldrich. 4-Phenylazophenyl methacrylate (AzoMA, A) was synthesized from methacryloyl chloride and 4-phenylazophenol, as previously described.[27] Methyl methacrylate (MMA, M) and benzyl methacrylate (BnMA, B) were purchased from Sigma-Aldrich and inhibitors were removed by passing through a neutral alumina column. [C_1mim][TFSI] was purchased from IoLiTec and subsequently purified via liquid−liquid extraction from water into dichloromethane (DCM) and then by stirring charcoal in the DCM solution, which was removed by filtration. The DCM was removed by rotary evaporation and the ionic liquid dried in a vacuum oven at 100 °C for 3 days. Ionic liquid purity was confirmed by visual inspection for a clear and colorless liquid, and by ^{1}H and ^{19}F NMR spectroscopy (Figure S2).

Polymer Synthesis. The polymers were synthesized via reversible addition-fragmentation chain transfer polymerization (RAFT). For all three block polymers, the same poly(methyl methacrylate) (PMMA) block was utilized. Three different chain extensions were performed to afford MBsA, MBA, and MAB. Reaction schemes can be found in the Supporting Information.

PMMA Block Synthesis (PMMA-CTA). A round-bottom flask (250 mL) was charged with purified methyl methacrylate (17.5 g, 174 mmol), 4,4′-azobis(4-cyanovaleric acid) (0.05 g, 0.19 mmol), 4-cyano-4-[(dodecylsulfanylthiocarbonyl)sulfanyl]pentanoic acid (0.78 g, 1.9 mmol), and 1,4-dioxane (42 mL). The system was degassed under argon for 25 min. The polymerization was run at 80 °C for 12 h, with the round-bottom flask placed in a preheated oil bath as the starting time, and then quenched by opening to air and placing on ice. The polymer was precipitated twice into cold methanol from DCM. The resulting polymer was dried overnight at 100 °C in a vacuum oven. The PMMA-CTA macroinitiator was characterized by size exclusion chromatography (SEC) and ^{1}H NMR spectroscopy (Figures S3 and S4), giving M_n = 9 kg/mol and $Đ$ = 1.06.

Synthesis of Poly(methyl methacrylate)-b-poly(benzyl methacrylate-stat-4-phenylazophenyl methacrylate) (MBsA). Purified PMMA-CTA (2 g, 0.21 mmol), purified benzyl methacrylate (3 g, 17 mmol), 4-phenylazophenyl methacrylate (0.24 g, 0.90 mmol), 4,4′-azobis(4-cyanovaleric acid) (0.006 g, 0.02 mmol), and 1,4-dioxane (9 mL) were stirred together in a septum-sealed pear-shaped flask (100 mL) and degassed with argon for 20 min. This pre-stirring was intended to mix the monomers thoroughly to achieve statistical incorporation of 4-phenylazophenyl methacrylate throughout the second block. The reaction was placed in an oil bath preheated to 75 °C and allowed to run for 18 h and then quenched by opening to air and placing on ice. The polymer was precipitated twice into cold methanol from DCM, and the resultant polymer was dried at 100 °C in the vacuum oven overnight. MBsA-CTA was characterized by size exclusion chromatography (SEC) and ^{1}H NMR spectroscopy (Figures S5 and S6), giving M_n = 22 kg/mol and $Đ$ = 1.05.

The statistical nature of the resulting block was assessed by calculating the average sequence length for each monomer based on literature reactivity ratios and initial concentrations. For BsA, r_{AzoMA} is 1.7 and r_{BnMA} is 0.8.[6] An average sequence length of 16 was calculated for BnMA and 1 for AzoMA at their initial concentrations of 1.9 and 0.1 M, respectively.[28] Therefore, the AzoMA monomers should be spaced out along the chain, and the resulting polymer can be assumed to be statistical.

CTA Removal. CTA end groups of all three block copolymers were removed by aminolysis followed by a Michael addition of methyl acrylate, as previously described.[20] In a representative reaction, MBsA-CTA (4 g, 0.18 mmol) was dissolved in tetrahydrofuran (70 mL) and stirred in a round-bottom flask (250 mL). Tris(carboxylethyl)-phosphine hydrochloride (0.078 g, 0.27 mmol) was dissolved in

https://doi.org/10.1021/acs.macromol.2c02113
Macromolecules XXXX, XXX, XXX−XXX

deionized water (0.7 mL) and added to the reaction. The system was degassed with argon for 20 min. *N*-propylamine (0.75 mL, 9 mmol) was added and stirred at room temperature for 5 h. Methyl acrylate (2.9 mL, 32 mmol) was subsequently added to the reaction and stirred overnight. Following quenching of the reaction, the THF was removed by rotary evaporation. The polymer was dissolved into DCM and precipitated twice into cold hexanes. The resultant polymer was dried in a vacuum oven at 100 °C for 2 days. CTA removal was confirmed by ^{1}H NMR spectroscopy, specifically by the disappearance of peaks between 1 and 1.5 ppm characteristic of the CTA (Figure S21). UV/vis spectroscopy was unable to be used due to interference from the azobenzene chromophore. All polymers were characterized by ^{1}H NMR spectroscopy and SEC, the results of which are listed in Table 1, and the spectra and chromatographic traces can be found in the Supporting Information.

Table 1. Polymer Characteristics

sample	M_n[a] (kg/mol)	M_w[a] (kg/mol)	$Đ$	f_{PMMA}[b]	n_{AzoMA}[b] (mol %)
MBsA	22	22	1.03	0.5	5
MBA	22	23	1.04	0.5	5
MAB	20	21	1.04	0.5	5

[a]Molar mass determined via SEC-MALS. [b]Determined via ^{1}H NMR spectroscopy.

Synthesis of Poly(methyl methacrylate)-b-poly(benzyl methacrylate)-b-poly(4-phenylazophenyl methacrylate) (MBA). First, the MB-CTA was synthesized by chain extending the PMMA-CTA with BnMA to yield MB-CTA, followed by a subsequent extension with 4-phenylazophenyl methacrylate to create MBA-CTA. Purified PMMA-CTA (2 g, 0.21 mmol), purified benzyl methacrylate (3 g, 17 mmol), 4,4′-azobis(4-cyanovaleric acid) (0.006 g, 0.02 mmol), and 1,4-dioxane (9 mL) were combined in a 20 mL scintillation vial sealed with a rubber septum. The system was degassed with argon for 20 min. The reaction was placed in an oil bath preheated to 75 °C and stirred for 12 h, and then quenched by opening the vial to air and placing on ice. The polymer was precipitated into cold methanol from DCM and dried in a vacuum oven at 100 °C overnight. MB-CTA was characterized by SEC and ^{1}H NMR spectroscopy (Figures S7 and S8), giving M_n = 18 kg/mol and $Đ$ = 1.1. The purified MB-CTA (2 g, 0.1 mmol) was placed in a scintillation vial with 1,4-dioxane (5 mL) and stirred to dissolve the polymer. 4-phenylazophenyl methacrylate (0.24 g, 0.9 mmol) was added to the vial. 4,4′-azobis(4-cyanovaleric acid) (0.003 g, 0.01 mmol) was dissolved in minimal 1,4-dioxane and added to the vial, before sealing with a rubber septum and degassing under argon for 20 min. The reaction was run for 3 h at 75 °C (with the round-bottom flask placed in a preheated oil bath), and quenched by opening to air and placing on ice. The polymer was precipitated into cold methanol from DCM and dried in a vacuum oven at 100 °C overnight. MBA-CTA was characterized by SEC and ^{1}H NMR spectroscopy (Figures S9 and S10), giving M_n = 22.7 kg/mol and $Đ$ = 1.07. The CTA was cleaved as described above, and the characterization data are listed in Table 1.

Synthesis of Poly(methyl methacrylate)-b-poly(4-phenylazophenyl methacrylate)-b-(benzyl methacrylate) (MAB). A similar procedure to the MBA synthesis was followed, where PMMA-CTA was first chain extended, in this case by adding the 4-phenylazophenyl methacrylate (0.24 g, 0.9 mmol, 3 h at 75 °C) and purified as previously described. MA-CTA was characterized by SEC and ^{1}H NMR spectroscopy (Figures S11 and S12), giving M_n = 12.1 kg/mol and $Đ$ = 1.1. The MA-CTA was then placed in a scintillation vial with benzyl methacrylate (1.14 g, 6.5 mmol), 4,4′-azobis(4-cyanovaleric acid) (0.002 g, 0.008 mmol), and 1,4-dioxane (4.5 mL); it was allowed to react for 19 h at 75 °C, and purified as described above. MAB-CTA was characterized by SEC and ^{1}H NMR spectroscopy (Figures S13 and S14), giving M_n = 20.9 kg/mol and $Đ$ = 1.07. The CTA was cleaved as described above, and the characterization data are listed in Table 1. The progression of each reaction to the next for MAB was tracked by SEC; chromatograms can be found in Figure S1b.

Materials Characterization. Proton nuclear magnetic resonance (^{1}H NMR) spectra of the polymers, the ionic liquids, and the AzoMA monomer were collected using a 400 MHz Bruker Avance III HD spectrometer, with deuterated DCM, deuterated dimethyl sulfoxide, and deuterated chloroform as solvents, respectively. Molar mass distributions for the polymers were obtained using SEC equipped with refractive index (Wyatt Optilab rEX) and multiangle light scattering detectors (Wyatt DAWN Helios II) with THF as the eluent. The dn/dc of the polymers in THF was calculated using a weighted average of the dn/dc values from M (0.086 mL/g), B (0.144 mL/g), and AzoMA (0.259 mL/g), where the weight percent monomer in the polymer was calculated from the ^{1}H NMR spectra.[20] All ^{1}H NMR spectra and SEC traces can be found in the Supporting Information.

Sample Preparation. Samples were prepared by a THF cosolvent method as previously described.[20] The polymer (0.35 or 0.5 g) and ionic liquid (0.65 or 0.5 g) were weighed into a 20 mL scintillation vial with a small stir bar. THF (10 mL) was added to the solution, which was stirred for at least 2 h. The solution was filtered through a PTFE filter (13 mm, 0.45 μm). The THF was then removed by nitrogen purge followed by the vials being placed in a vacuum oven at 100 °C overnight. Samples were stored in a desiccator under vacuum.

Small-Angle X-ray Scattering. Small-angle X-ray scattering (SAXS) was performed at Sector 5-ID-D of the Advanced Photon Source at Argonne National Lab. The samples were loaded into aluminum sample pans, then dried in a vacuum oven at 100 °C overnight prior to loading into a glovebox, and sealed hermetically in an argon glovebox. Measurements were taken upon heating from 30 to 175 °C with about 10 min annealing at each temperature. The sample-to-detector distance was fixed at 7.5 m, the beam energy was 17.5 keV (wavelength λ = 0.7293 Å), and SAXS data were collected by a Rayonix area detector. The isotropic two-dimensional (2D) data were reduced by azimuthal integration to give intensity as a function of the scattering wave vector, q. SAXS measurements were taken in the dark.

Small-Amplitude Oscillatory Shear Photorheology. Small-amplitude oscillatory shear photorheology was performed on a TA Instruments Discovery HR3 rheometer fitted with an electrically heated upper plate (40 mm dia.) and a quartz lower plate (20 mm dia.). An in-depth description of this setup, including that of the UV lower plate attachment, was provided in previous work.[20,22] An Omnicure S1500 mercury arc lamp was used for irradiation, with 365 and 400−500 nm wavelength filters to allow for UV and visible wavelength penetration, respectively. Samples were measured with a gap of less than 300 μm. Temperature sweeps were performed from 30 to 150 °C at a frequency of 1 rad/s and a strain of 1%. Strain sweeps were performed at 30 and 150 °C to ensure that the measurements were taken in the linear viscoelastic regime. Frequency sweeps were also performed at various temperatures after the initial temperature sweeps, with annealing at 100 °C for 30 min prior to measurements in the dark (no irradiation and a shield in place) and annealing at 30 °C under UV radiation for 30 min prior to measurements under UV illumination with the same shield in place. For all cases, T_{ODT} is taken as the point where the storage modulus, G', is equal to the loss modulus, G'', or where $\tan(\delta) = G''/G' = 1$; $\tan(\delta) > 1$ indicates a disordered sample and $\tan(\delta) < 1$ an ordered state.

RESULTS AND DISCUSSION

Three block copolymers of differing architecture, but constant composition, were synthesized: one incorporated the azobenzene statistically within the BnMA block (MBsA), one with the AzoMA as an end-block (MBA), and one with the AzoMA as a midblock (MAB). All three block copolymers used the same PMMA macro-CTA and thus all have the same solvophilic block. The AzoMA content was maintained at 5 mol% relative to BnMA, and the only difference in the polymerization was

https://doi.org/10.1021/acs.macromol.2c02113
Macromolecules XXXX, XXX, XXX−XXX

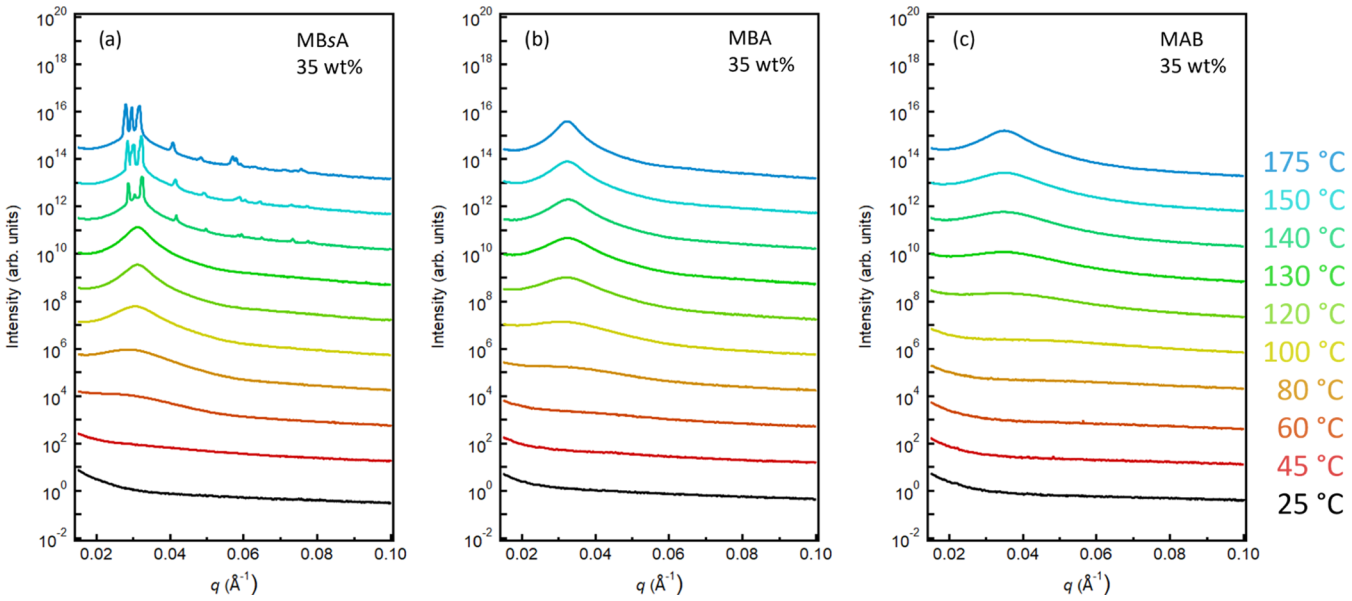

Figure 2. SAXS patterns for all three polymers at 35 wt % in [C1mim][TFSI]. Patterns are shifted vertically for clarity. (a) MBsA shows an ODT near 140 °C, to hexagonally close-packed spheres (HCP). (b) MBA shows peak sharpening at 175 °C but remains disordered. (c) MAB remains disordered at all temperatures.

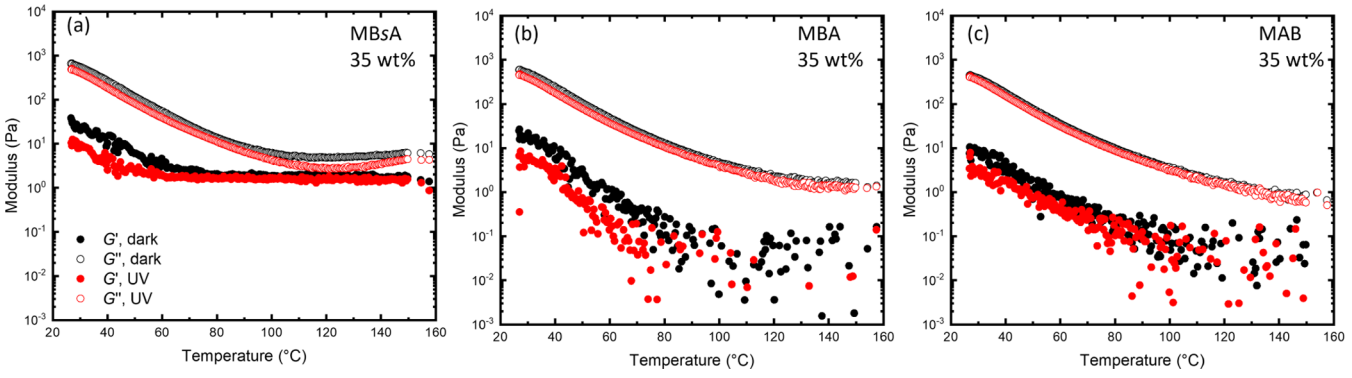

Figure 3. SAOS temperature sweep plots for MBsA and MBA at 35 wt % in [C_1mim][TFSI]. In each panel, black symbols indicate the samples in the dark, while red symbols are under UV irradiation. (a) MBsA. (b) MBA, (c) MAB. Gap: <300 μm, strain: 1%, frequency: 1 rad/s, temperature ramp: 3 °C/min, UV intensity: 50 mW/cm^2.

the order of addition of AzoMA. The characteristics of the synthesized polymers are listed in Table 1.

To analyze the influence of the azobenzene location on the polymer, the major considerations are T_{ODT} (SAXS, rheology), the ordered state formed (SAXS), and the difference in linear viscoelastic behavior in the dark and under UV irradiation (photorheology). For SAXS, samples were analyzed over a temperature range from 30−175 °C at the Advanced Photon Source at Argonne National Lab. Microphase separation within a disordered state is characterized in SAXS by a broad peak, while ordering is characterized by the primary scattering peak width narrowing and the appearance of subsequent Bragg peaks, which can be indexed to specific symmetries.[29]

35 wt % Polymer in Solution. Initially, 35 wt % solutions of all three polymers in [C_1mim][TFSI] were compared using SAXS (Figure 2). As demonstrated previously, a spherical particle phase is expected at 35 wt % for a symmetric MBsA in [C_1mim][TFSI].[20] Across the three samples, MBsA (Figure 1a) had the lowest T_{ODT} at 130 °C. Above this temperature, Bragg scattering peaks indexed to hexagonally close-packed spheres (HCP), indicated by the (100), (020), and (101) indices situated close together at low q (Figure S22a). The unexpected prevalence of HCP, rather than the more typical BCC, in ionic liquid solutions with PBnMA-based block polymers, was noted previously.[22] Microphase separation, found upon heating in this lower critical ordering transition solution, is indicated by a broad disordered peak, in this case at 60 °C (Figure 2a, red-orange curve). By locating the photoactive monomer at the end of the chain in MBA (Figure 2b), the onset of microphase separation is observed at 80 °C, as indicated by the broad disordered peak (orange curve). This is approximately 20 °C higher than for MBsA; however, no ordering is observed over the temperature range studied. Based on the progression of peak narrowing observed from MBsA, the T_{ODT} in MBA could be expected at about 185 °C. The dispersion of A through the responsive block in MBsA causes the LCOT of the polymer to be lower than that of the pure PBnMA polymer due to the presence of the insoluble azobenzene. Therefore, its LCOT is lower than the perceived LCOT of MBA due to the microphase separation of the triblock occurring in two steps: first the A block microphase separates, then B. The LCOT of MBA could be decreased by

https://doi.org/10.1021/acs.macromol.2c02113
Macromolecules XXXX, XXX, XXX−XXX

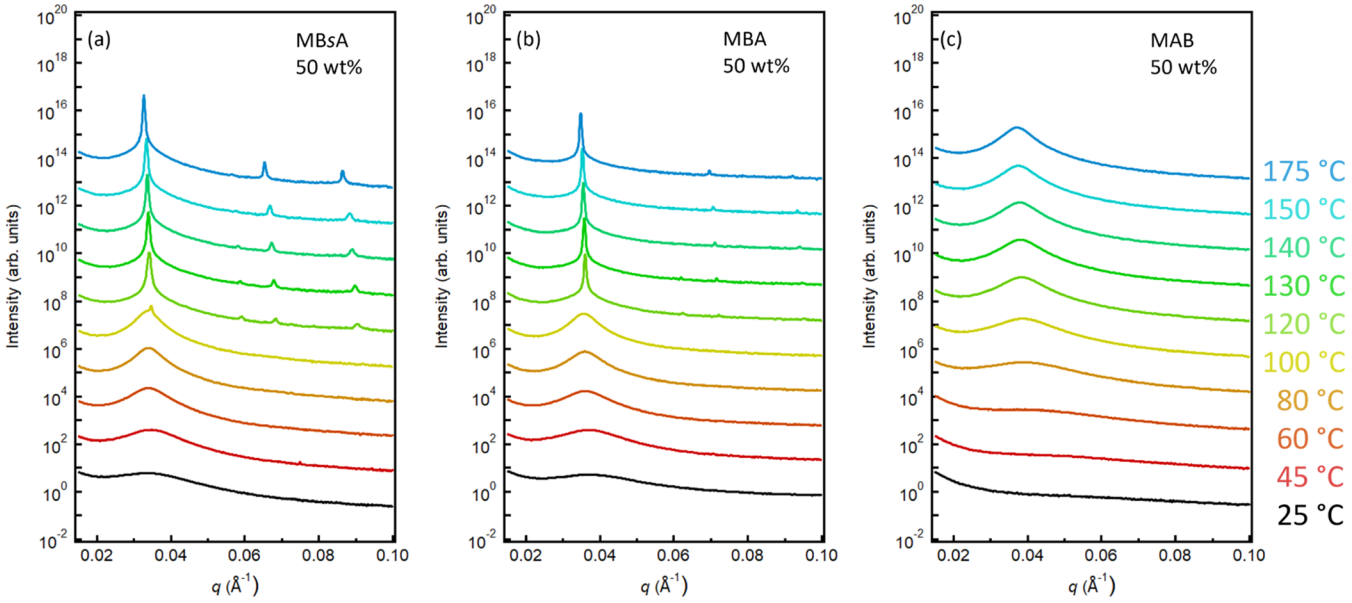

Figure 4. SAXS patterns for all three polymers at 50 wt % in [C_1mim][TFSI]. Patterns are shifted for clarity. (a) MBsA shows a disorder−order transition at 120 °C to hexagonally packed cylinders (HEX). (b) MBA orders around the same temperature, 120 °C, to hexagonally packed cylinders. (c) MAB remains disordered at all temperatures.

increasing the molar mass of the A block, as a critical point would be reached where the A block drives the overall microphase separation rather than the B block. For MAB, where the photoactive monomer is between the M and B blocks, the onset of microphase separation is not observed until 120 °C (Figure 2c, light green curve). Also, no ordering is observed over the temperature range studied. As the principal peak is still broad and quite weak at 175 °C, resembling that of MBsA at 100 °C, it can be assumed that a further increase in temperature by at least 40 °C would be required to reach the T_{ODT}. The difference in T_{ODT} between two 60 kg/mol PMMA-*b*-P(BnMA-*s*-AzoMA) polymers, one with no azobenzene and one with 5 mol % AzoMA statistically copolymerized in the PBnMA, at 35 wt % in [C_1mim][TFSI] was 80 °C, a slightly larger difference than that between MAB and MBsA here.[20] This suggests that the midblock AzoMA is partially shielded from the solvent, and ordering will instead be driven by the PBnMA block.

In rheology, the ODT is typically indicated by a crossover between G' and G'' at low frequencies, or at least a sharp change in G'. The difference in mechanical behavior in the dark and under UV irradiation is of interest, as these materials are intended to be both thermo- and photoresponsive. A significant difference in behavior, such as an increase in T_{ODT} with UV, is therefore desired. Rheological measurements at 35 wt % confirmed the persistence of disorder over all temperatures in the MBA and MAB samples (Figure 3b,c). For MBsA, G' and G'' approach a common value of 3 Pa at 120 °C, but no crossover between G' and G'' (the rheological indication of an ODT) is observed at 140 °C, the T_{ODT} from SAXS (Figure 3a). As 140 °C is approaching the upper-temperature limit of the rheometer, the crossover may not be easily seen, as observed with s-MBsA$_5$ in [C_4mim][TFSI].[20] Lowering the frequency of the temperature sweep to 0.1 rad/s did not increase the signal due to ordering (Figure S23). There is no significant change in behavior under UV irradiation (red symbols) from in the dark (black symbols) for all three samples. For both MAB and MBA, rheology reflects a disordered, liquid-like state across the observable temperature range. The UV irradiation also did not have an impact on the rheological behavior of the 35 wt % solutions. As both MBA and MAB are already disordered over the temperatures of interest in both SAXS and rheology, this behavior was expected. For MBsA, the lack of photoresponse was surprising. However, the T_{ODT} approaching the temperature limit of the instrument in the dark indicates that any change in UV would occur at even higher temperatures, making such behavior unobservable with this technique. As only one of the three polymers ordered at 35 wt %, a higher concentration of polymer was examined to be able to compare the ordering behavior.

50 wt % Polymer in Solution. The concentration of polymer in ionic liquid was increased to 50 wt % to assess whether ordering behavior could be observed across all three polymers. Assuming 100% exclusion of solvent from the core, the core volume fraction can be estimated to be $f_{eff,B} \geq 0.22$ for all three polymers, which would typically coincide with the formation of hexagonally packed cylinders (HEX).[20,30] Figure 4 shows SAXS patterns from 30 to 175 °C. Again, the MBsA ordered first at 120 °C to HEX (Figure 4a), with the appropriate indexing in Figure S22b. For MBA, the higher concentration of AzoMA at 50 wt % was able to drive ordering to HEX (Figure 4b, indexing in Figure S22c). Both the MBsA and the MBA samples are already microphase-separated at room temperature. The principal peaks, q^*, are also located in similar locations, about 0.034 Å^{-1}, indicating that the domain spacing is similar. The progression of the principal peaks was compared in Figure S26. MAB continued to be disordered over all temperatures, but microphase separation is observed at 60 °C (Figure 4c). As the AzoMA was at the center of the polymer in MAB, ordering could be impeded by chain crowding and attendant difficulties with subsequent rearrangement upon PBnMA microphase separation, leading to higher barriers due to the additional A/B interface and restricted diffusion of the particles. This results in MAB behaving more like PMMA-*b*-PBnMA. Although all three polymers are at

https://doi.org/10.1021/acs.macromol.2c02113
Macromolecules XXXX, XXX, XXX−XXX

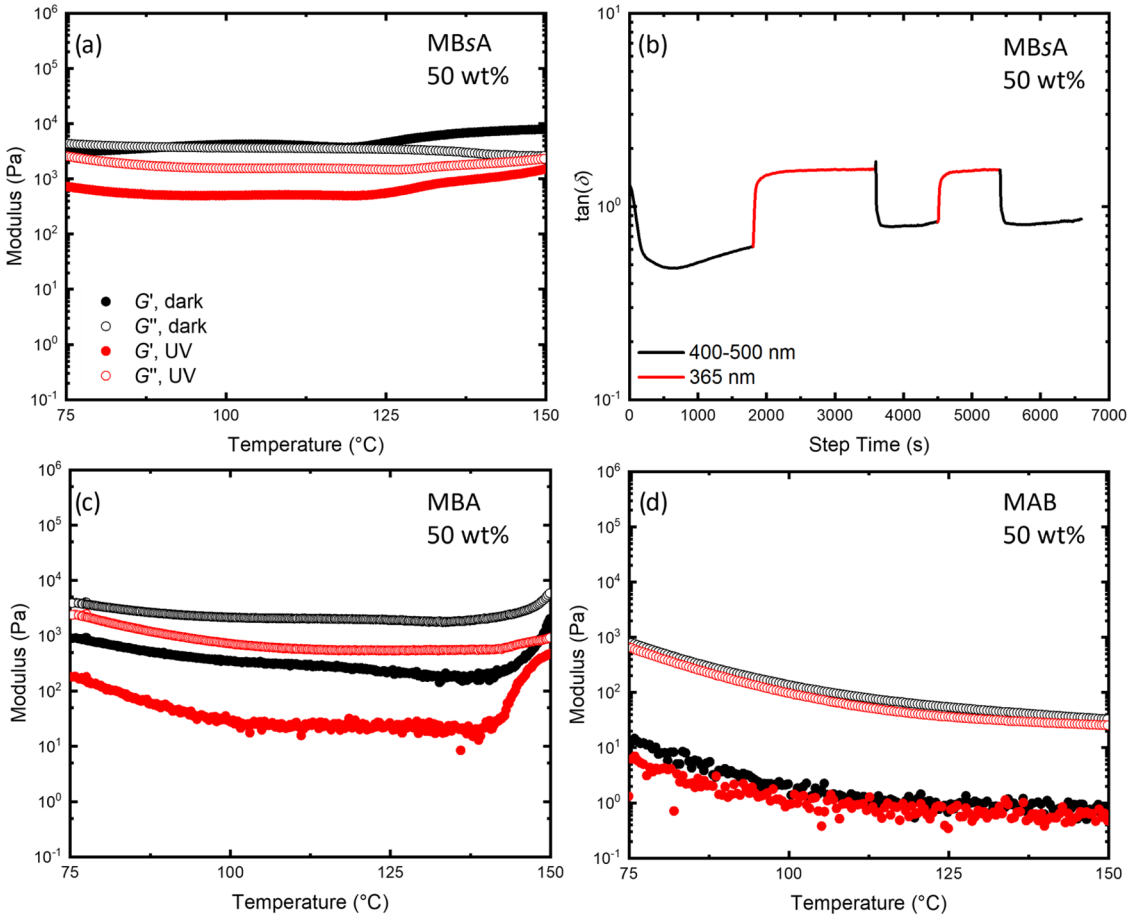

Figure 5. SAOS temperature sweep plots at 50 wt % in [C_1mim][FSI]. In each panel, black symbols indicate the samples in the dark, while red symbols are under UV irradiation. (a) MBsA, ODT in the dark (black) is 90 °C, under UV (red) is above 150 °C. (b) SAOS time sweep plot for MBsA in [C_2mim][TFSI]. Temperature was kept constant at 130 °C and the wavelength of the light source was alternated between 365 nm (red curves) and 400−500 nm (black curves) by changing a light filter. Tan(δ) < 1 indicates order; tan(δ) > 1 indicates disorder. Transitions are sharp, indicating clean switching between order and disorder. (c) For MBA, no ODT is observed in rheology; however, upon UV irradiation, the modulus drops, indicating that the chain end is now more solvophilic. (d) MAB is disordered over all temperatures explored, with no change under UV irradiation. Gap: <300 μm, strain: 1%, frequency: 1 rad/s, temperature ramp: 3 °C/min, UV intensity: 50 mW/cm^2.

cylinder-forming concentrations, MAB did not order below 175 °C.

Photo-rheological measurements were taken on the 50 wt % samples, with temperature sweeps from 75 to 150 °C (Figure 5). The samples were glassy, so for the protection of the quartz lower plate, the temperature was restricted to be at or above 75 °C and were loaded at 100 °C. The MBsA sample at 50 wt % showed ordering above 125 °C (Figure 5a), where G' increases above G''. While no clear crossover was observed, as G' and G'' had similar values up until 125 °C, the deviation between the two indicates that ordering occurred around that temperature. In this case, the T_{ODT} was consistent between SAXS and rheology. At 130 °C, photo-triggering of the ODT was successful over multiple cycles by varying the wavelength of light irradiating the sample from 365 nm to the 400−500 nm range. The results of the cycling can be seen in Figure 5b, in a rheological time sweep where the loss tangent best represented the change from order (tan(δ) <1, black curves) disorder (tan(δ) > 1, red curves). The ODT reversed almost immediately upon changing the filter, indicating a facile and reversible transition.

For MBA (Figure 5c), no crossover is observed, yet a sharp increase in modulus occurred at 140 °C, slightly both the microphase separation and ordering temperatures seen in SAXS (130 °C). A significant change was observed upon UV irradiation, with the modulus dropping by an order of magnitude. Hysteresis between the heating and cooling traces was observed for both MBsA and MBA in the rheological properties (Figure S23). For MBA upon cooling, the modulus returned to the lower value at 127 °C, which is closer to the ODT observed in SAXS (Figure S23b). Hysteresis in long-range ordering reflects a nucleation barrier. Therefore, the disordering temperature, in this case upon cooling, is found to be closer to the thermodynamic binodal curve. This behavior may be due to the frequency being 1 rad/s during the temperature sweep. Frequency sweeps at 130 °C (Figure S25) indicate that at 1 rad/s, MBsA showed $G' > G''$, while MBA has $G' < G''$. As shown in Figure S25b, a frequency over 100 rad/s would be necessary to observe ordering in MBA by rheology, which is impractical. As SAXS is not frequency-dependent, the ordering was easily observed. MAB continued to show no signs of ordering over the temperatures accessible in the rheometer (Figure 5d), and no difference in behavior was observed under UV radiation, consistent with the SAXS results.

Comparison across Concentrations. Microphase separation is governed by the interaction energy between the blocks and between each block and the solvent. This

https://doi.org/10.1021/acs.macromol.2c02113
Macromolecules XXXX, XXX, XXX−XXX

interaction is represented by the Flory–Huggins interaction parameter, χ. For MBsA, three χ values influence the behavior: $\chi_{M\text{-}BsA}$, $\chi_{M\text{-}IL}$, and $\chi_{BsA\text{-}IL}$. $\chi_{BsA\text{-}IL}$ and $\chi_{M\text{-}BsA}$ can be combined into an effective $\chi_{M/IL\text{-}BsA}$, which is both temperature- and light-dependent. The distribution of the AzoMA through the PBnMA causes $\chi_{M/IL\text{-}BsA}$ to be larger than for PBnMA with PMMA and [C_1mim][TFSI]. This encouraged microphase separation at a lower temperature than PMMA-*b*-PBnMA and ordering into cylinders at 50 wt %, or spheres, at 35 wt %. For the triblock polymers, six χ values are involved, one between each component. $\chi_{IL\text{-}A}$ is photoresponsive and $\chi_{IL\text{-}B}$ is thermoresponsive. For MBA, the terminal A block drives ordering, as *trans*-AzoMA is insoluble in [C_1mim][TFSI] ($\chi_{IL\text{-}A} \gg 0.5$ in the dark). In the dark, the AzoMA microphase separates and starts to form cylinders, which become denser as the PBnMA block also microphase separates. For MAB, the most solvophobic block is in the middle of the polymer. If the AzoMA was driving microphase separation, forming spheres or cylinders would require chain crowding for both B and M blocks. Alternatively, the AzoMA midblock could be shielded from the solution by the much larger blocks on either side, and thus the behavior would resemble PMMA-*b*-PBnMA. In either case, the chains were observed to aggregate and microphase-separate, but did not order below 175 °C.

If MBsA were to create a blocky polymer, with the AzoMA monomer incorporated preferentially earlier in the polymerization, the resulting monomer sequence would be closer to MAB, and therefore those two polymers would behave similarly. However, the results demonstrated that this was not the case. MAB was consistently disordered over all temperatures analyzed, while MBsA readily ordered into indexable states at both concentrations analyzed. In addition, the overall behavior of MBsA did not match that of MBA, especially with respect to concentration changes. Considering the literature reactivity ratios, the average path length for BnMA was 16 and that for AzoMA was 1, so the AzoMA is likely well spaced along the chain. Overall, we can assume that, with this preparation method, MBsA had azobenzene reasonably dispersed through the BnMA block. With the lack of order for MAB, it will not be considered further.

To compare MBsA to MBA as photo- and thermoresponsive materials, their behavior in photo-SAOS is compared. At 50 wt %, UV irradiation changed the behavior of both MBsA and MBA. For MBA, the modulus dropped by an order of magnitude, indicating that $\chi_{IL\text{-}A}$ changed significantly upon UV irradiation, leading to a lower overall modulus for the sample. Therefore, the AzoMA end-block in the more polar *cis* state was much better solvated and no longer driving microphase separation. A small decrease in modulus was observed for MBsA upon UV irradiation, and a crossover between G' and G'' was observed in the dark at 125 °C. ODT triggering with UV light was possible at 130 °C for MBsA (Figure 5b). Photo-based ODTs were not accessible on the rheometer for MBA, as no ordering was observed in the dark. Therefore, the statistical copolymerization of AzoMA through the PBnMA block leads to a useful photo- and thermoresponsive material, while MBA showed ordering in SAXS at 50 wt % but not in the rheology. The data are summarized in Table 2.

Table 2. Summary of Transitions

concentration (wt %)	polymer	microphase separation (°C)	T_{ODT} (°C)	ordered state
35	MBsA	60	130	HCP
	MBA	80		DIS
	MAB	120		DIS
50	MBsA	<25	120	HEX
	MBA	<25	130	HEX
	MAB	60		DIS

CONCLUSIONS

This work focuses on investigating the impact of the location of a photoactive monomer within a thermoresponsive polymer. Our previous research focused on statistically polymerized solutions of poly(methyl methacrylate)-*block*-poly(benzyl methacrylate-stat-4-phenylazophenyl methacrylate) in ionic liquids. We prepared three polymers to compare placing the azobenzene either in the middle or at the end of the polymer, relative to the statistical version. The position of the azobenzene matters for the overall behavior of the polymer. Statistical incorporation was best for controlling the order–disorder transition with light, as well as for forming well-defined ordered states at multiple polymer concentrations.

ASSOCIATED CONTENT

Supporting Information

The Supporting Information is available free of charge at https://pubs.acs.org/doi/10.1021/acs.macromol.2c02113.

Synthetic schemes for the preparation of all polymers; proton and fluorine nuclear magnetic resonance spectra and size exclusion chromatographs for polymer and ionic liquid characterization; rheology plots illustrating triggering ODTs with light; hysteresis on heating/cooling; comparison of temperature sweeps at various frequencies; frequency scans for all polymer solutions at various temperatures; and q^* vs temperature plot from SAXS (PDF)

AUTHOR INFORMATION

Corresponding Author

Timothy P. Lodge – *Department of Chemistry and Department of Chemical Engineering and Materials Science, University of Minnesota, Minneapolis, Minnesota 55455, United States;* orcid.org/0000-0001-5916-8834; Email: lodge@umn.edu

Author

Claire L. Seitzinger – *Department of Chemistry, University of Minnesota, Minneapolis, Minnesota 55455, United States;* orcid.org/0000-0002-4700-9964

Complete contact information is available at: https://pubs.acs.org/10.1021/acs.macromol.2c02113

Notes

The authors declare no competing financial interest.

ACKNOWLEDGMENTS

This work was supported through NSF Polymers Program, Awards DMR-1797578 and DMR-2103630. The rheological measurements were carried out in the College of Science and Engineering Polymer Characterization Facility, University of Minnesota, which has received capital equipment funding from the National Science Foundation through the UMN MRSEC under Award Number DMR-201140. The SAXS measurements were performed at the DuPont-Northwestern-Dow Collaborative Access Team (DND-CAT) located at the Sector

5 of the Advanced Photon Source (APS). DND-CAT is supported by E.I. DuPont de Nemours & Co., the Dow Chemical Company, and Northwestern University. Use of the APS, an Office of Science User Facility operated for the U.S. DOE Office of Science by Argonne National Laboratory, was supported by the U.S. DOE under contract no. DE-AC02-06CH11357. The authors thank S. Piril Ertem for editing, David Giles for discussions about the rheology, and Aaron Lindsay and Andreas Mueller for writing and refining an Igor code for indexing SAXS patterns (https://doi.org/10.13020/9m8p-pv93).

REFERENCES

(1) Bertrand, O.; Gohy, J. F. Photo-Responsive Polymers: Synthesis and Applications. *Polym. Chem.* **2017**, *8*, 52−73.
(2) Zhao, Y. Photocontrollable Block Copolymer Micelles: What Can We Control? *J. Mater. Chem.* **2009**, *19*, 4887−4895.
(3) Dai, S.; Ravi, P.; Tam, K. C. Thermo- and Photo-Responsive Polymeric Systems. *Soft Matter* **2009**, *5*, 2513−2533.
(4) Ciardelli, F.; Pieroni, O.; Fissi, A.; Carlini, C.; Altomare, A. Photoresponsive Optically Active Polymers—a Review. *Br. Polym. J.* **1989**, *21*, 97−106.
(5) Irie, M. Photoresponsive Polymers. In *New Polymer Materials*; Springer-Verlag: Berlin/Heidelberg, 1990; Vol. *94*, pp 27−67.
(6) Ueki, T.; Yamaguchi, A.; Ito, N.; Kodama, K.; Sakamoto, J.; Ueno, K.; Kokubo, H.; Watanabe, M. Photoisomerization-Induced Tunable LCST Phase Separation of Azobenzene-Containing Polymers in an Ionic Liquid. *Langmuir* **2009**, *25*, 8845−8848.
(7) Ueki, T.; Usui, R.; Kitazawa, Y.; Lodge, T. P.; Watanabe, M. Thermally Reversible Ion Gels with Photohealing Properties Based on Triblock Copolymer Self-Assembly. *Macromolecules* **2015**, *48*, 5928−5933.
(8) Ueki, T.; Yamaguchi, A.; Watanabe, M. Unlocking of Interlocked Heteropolymer Gel by Light: Photoinduced Volume Phase Transition in an Ionic Liquid from a Metastable State to an Equilibrium Phase. *Chem. Commun.* **2012**, *48*, No. 5133.
(9) Ye, Q.; Huo, M.; Zeng, M.; Liu, L.; Peng, L.; Wang, X.; Yuan, J. Photoinduced Reversible Worm-to-Vesicle Transformation of Azo-Containing Block Copolymer Assemblies Prepared by Polymerization-Induced Self-Assembly. *Macromolecules* **2018**, *51*, 3308−3314.
(10) Wang, C.; Ma, X.; Kitazawa, Y.; Kobayashi, Y.; Zhang, S.; Kokubo, H.; Watanabe, M. From Macromolecular to Small-Molecular Triggers: Facile Method toward Photoinduced LCST Phase Behavior of Thermoresponsive Polymers in Mixed Ionic Liquids Containing an Azobenzene Moiety. *Macromol. Rapid Commun.* **2016**, *37*, 1960−1965.
(11) Ueki, T. Stimuli-Responsive Polymers in Ionic Liquids. *Polym. J.* **2014**, *46*, 646−655.
(12) Irie, M.; Tanaka, H. Photoresponsive Polymers. 5. Reversible Solubility Change of Polystyrene Having Azobenzene Pendant Groups. *Macromolecules* **1983**, *16*, 210−214.
(13) Hartley, G. S. The Cis-Form of Azobenzene. *Nature* **1937**, *140*, 281.
(14) Dahn, V. H.; Castelmurl, H. Uber Die Absorptionsspektren von Polyazoverbindungen. *Helv. Chim. Acta* **1952**, *36*, 638−645.
(15) Kumar, G. S.; Neckers, D. C. Photochemistry of Azobenzene-Containing Polymers. *Chem. Rev.* **1989**, *89*, 1915−1925.
(16) Ueno, K. Synthesis and Ultraviolet Absorption Spectra of Polyazobenzenes. *J. Am. Chem. Soc.* **1952**, *74*, 4508−4511.
(17) Ueno, K.; Akiyoshi, S. Polyazobenzenes. II. Synthesis and Ultraviolet Absorption Spectra of Polyazobenzenes Containing Nitro, Amino and Hydroxyl Groups. *J. Am. Chem. Soc.* **1954**, *76*, 3667−3670.
(18) Ueno, K. Polyazobenzenes. III. Infrared Absorption Spectra of Some Polyazobenzenes. *J. Am. Chem. Soc.* **1957**, *79*, 3205−3208.
(19) Adhikari, B.; Yamada, Y.; Yamauchi, M.; Wakita, K.; Lin, X.; Aratsu, K.; Ohba, T.; Karatsu, T.; Hollamby, M. J.; Shimizu, N.; Takagi, H.; Haruki, R.; Adachi, S. I.; Yagai, S. Light-Induced Unfolding and Refolding of Supramolecular Polymer Nanofibres. *Nat. Commun.* **2017**, *8*, No. 15254.
(20) Seitzinger, C. L.; Hall, C. C.; Lodge, T. P. Photoreversible Order−Disorder Transitions in Block Copolymer/Ionic Liquid Solutions. *Macromolecules* **2022**, *55*, 3811−3820.
(21) Hall, C. C.; Rivera, C. A.; Lodge, T. P. The Effect of Light Penetration Depth on the LCST Phase Behavior of a Thermo- and Photoresponsive Statistical Copolymer in an Ionic Liquid. *J. Polym. Sci., Part A: Polym. Chem.* **2019**, *57*, 281−287.
(22) Hall, C. C.; Lodge, T. P. Photoreversible Order−Disorder Transition in an Ionic Liquid Solvated Block Polymer. *ACS Macro Lett.* **2019**, *8*, 393−398.
(23) Wang, C.; Hashimoto, K.; Zhang, J.; Kobayashi, Y.; Kokubo, H.; Watanabe, M. Micellization/Demicellization Self-Assembly Change of ABA Triblock Copolymers Induced by a Photoswitchable Ionic Liquid with a Small Molecular Trigger. *Macromolecules* **2017**, *50*, 5377−5384.
(24) Wang, C.; Hashimoto, K.; Tamate, R.; Kokubo, H.; Morishima, K.; Li, X.; Shibayama, M.; Lu, F.; Nakanishi, T.; Watanabe, M. Viscoelastic Change of Block Copolymer Ion Gels in a Photo-Switchable Azobenzene Ionic Liquid Triggered by Light. *Chem. Commun.* **2019**, *55*, 1710−1713.
(25) Wang, C.; Hashimoto, K.; Tamate, R.; Kokubo, H.; Watanabe, M. Controlled Sol−Gel Transitions of a Thermoresponsive Polymer in a Photoswitchable Azobenzene Ionic Liquid as a Molecular Trigger. *Angew. Chem., Int. Ed.* **2018**, *57*, 227−230.
(26) Wang, C.; Hashimoto, K.; Tamate, R.; Kokubo, H.; Watanabe, M. Controlled Sol-Gel Transitions of a Thermoresponsive Polymer in a Photoswitchable Azobenzene Ionic Liquid as a Molecular Trigger. *Angew. Chem.* **2018**, *130*, 233−236.
(27) Lundin, F.; Hansen, H. W.; Adrjanowicz, K.; Frick, B.; Rauber, D.; Hempelmann, R.; Shebanova, O.; Niss, K.; Matic, A. Pressure and Temperature Dependence of Local Structure and Dynamics in an Ionic Liquid. *J. Phys. Chem. B* **2021**, *125*, 2719−2728.
(28) Lodge, T. P.; Hiemenz, P. C.; *Polymer Chemistry*, 3rd ed.; CRC Press, 2020.
(29) Bates, F. S.; Fredrickson, G. H. Block Copolymers—Designer Soft Materials. *Phys. Today* **1999**, *52*, 32−38.
(30) Hanley, K. J.; Lodge, T. P.; Huang, C.-I. Phase Behavior of a Block Copolymer in Solvents of Varying Selectivity. *Macromolecules* **2000**, *33*, 5918−5931.

https://doi.org/10.1021/acs.macromol.2c02113
Macromolecules XXXX, XXX, XXX−XXX